

# TOC Entry

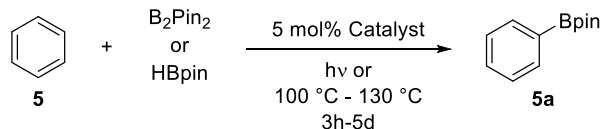
## The Functionalization of Benzene by Boranes

### Using Trispyrazolylborate Complexes

Andrew J. Vetter, Tarah A. DiBenedetto<sup>‡</sup>, Mikhaila D. Ritz<sup>‡</sup> and William D. Jones\*

Department of Chemistry, University of Rochester, Rochester, NY 14627

TOC Graphic



The investigation of four trispyrazolylborate complexes of rhodium(I) and iridium(I) are examined for arene borylation catalysis using pinic平borane and dipinic平borane, with  $\text{Tp}'\text{Rh}(\text{C}_2\text{H}_4)_2$  showing the best activity.

# The functionalization of benzene by boranes using trispyrazolylborate complexes

Andrew J. Vetter, Tarah A. DiBenedetto<sup>#</sup>, Mikhaila D. Ritz<sup>#</sup> and William D. Jones\*

Department of Chemistry, University of Rochester, Rochester, NY 14627

Keywords: rhodium, iridium, trispyrazolylborate, borylation, arenes

**ABSTRACT:** The catalytic C-H activation and borylation of arenes by trispyrazolylborate complexes is reported. Trispyrazolylborate rhodium and iridium complexes have been previously shown to activate a variety of C-H bonds. Here, we show the catalytic borylation of arenes by the trispyrazolylborate ethylene complexes  $\text{Tp}'\text{Rh}(\text{C}_2\text{H}_4)_2$ , and  $\text{Tp}'\text{Ir}(\text{C}_2\text{H}_4)_2$ .

## 1. Introduction

Organoboron compounds are highly relevant in both the pharmaceutical and synthetic fields, as they are used in numerous transformations such as metal catalyzed cross couplings, conjugate additions, and oxidative aminations [1,2]. These boron containing compounds are commonly synthesized from aryl halides via Grignard or lithium reagents, or directly by the metal catalyzed reaction of aryl or alkyl halides with boron reagents. While effective, these methods increase synthetic overhead and rely on the accessibility of halide precursors [3]. An alternative approach is the direct borylation of C-H bonds, which avoids the need for prefunctionalized starting materials and allows for a more atom economical strategy for the synthesis of borylated products [3].

The importance of these compounds has driven the development of new methodologies for direct arene borylation over the last few decades. Hartwig reported in 1995 a photochemical borylation of arenes and olefins using  $\text{CpFe}(\text{CO})_2(\text{Bcat})$ ,  $\text{Mn}(\text{CO})_5(\text{Bcat})$ , and  $\text{W}(\text{CO})_5(\text{Bcat})$  (cat = catechol) [4]. This photochemistry was extended to alkanes stoichiometrically using  $\text{Cp}^*\text{W}(\text{CO})_3(\text{Bcat})$  [5], and catalytically using  $\text{Cp}^*\text{Re}(\text{CO})_3$  [6]. In 1999, Smith and coworkers reported the first catalytic borylation of arenes using an iridium pentamethylcyclopentadienyl catalyst [7]. Further improvements have been made by Ishiyama, Miyaura, and Hartwig by using iridium precursors in combination with bidentate ligands [8,9]. Direct arene borylation has since been catalyzed by rhodium, platinum, and other iridium catalysts [10-13], as well as first row transition metals such as cobalt [14], nickel [2], and iron [15,16]. Most recently, Farha has shown that an iridium catalyst can be supported in a MOF to achieve arene borylation with  $\text{B}_2\text{pin}_2$  (pin = pinacol) [17]. The development of these and other systems have been reviewed in 2010 [3].

The direct borylation of arenes is a fundamental tool for synthetic chemistry that is reliant on the activation of C-H bonds [18]. Hartwig and coworkers have shown the catalytic borylation of alkanes and arenes using a  $[\text{Cp}^*\text{M}(\text{C}_2\text{H}_4)_2$  ( $\text{M} = \text{Rh, Ir}$ ) catalyst [19]. Previous work has shown that the isoelectronic  $\text{Tp}'\text{Rh}(\text{C}_2\text{H}_4)_2$  and  $\text{Tp}'\text{Ir}(\text{C}_2\text{H}_4)_2$  complexes are able to activate both alkane and arene C-H bonds [20-24], but have not been investigated for the catalytic borylation of arenes. The success

of the analogous pentamethylcyclopentadienyl catalysts offers an opportunity for the development of a catalytic borylation based on the trispyrazolylborate scaffold.

## 2. Results and discussion

### 2.1. Borylation with $\text{Tp}'\text{Rh}(\text{CNR})(\eta^2\text{-PhN=CNR})$

The borylation of benzene using various trispyrazolylborate metal complexes was studied (Fig. 1). Our initial investigation began with catalyst **1**  $\text{Tp}'\text{Rh}(\text{CNR})(\eta^2\text{-PhN=CNR})$  ( $\text{R} = \text{neopentyl}$ ), which when irradiated in the presence of benzene is known to form the C-H oxidative addition product [25].

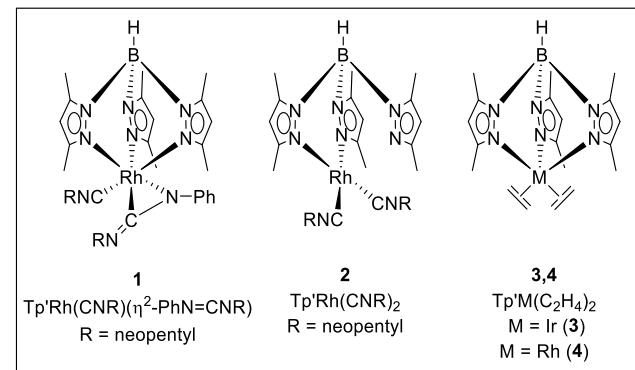


**Fig. 1. Trispyrazolylborate catalysts**

Catalyst **1** was irradiated at room temperature in the presence of  $\text{B}_2\text{pin}_2$  ( $\text{B}_2\text{pin}_2 = \text{bis}(\text{pinacolato})\text{diborane}$ ) and benzene for 10 minutes, resulting in the bleaching of the bright yellow solution. However, no formation of desired product  $\text{PhBpin}$  (**5a**) was observed by GC, and only starting materials were present. The C-H activation product  $\text{Tp}'\text{Rh}(\text{CNR})(\text{C}_6\text{H}_5)\text{H}$  (**1a**) was observed as the only metal complex by NMR spectroscopy. Extended irradiation also did not result in formation of any of the desired product.

Catalysis with **1** was also attempted thermally. A mixture of catalyst **1**,  $\text{B}_2\text{pin}_2$ , and benzene was heated for 4.5 h at 115 °C. Analogous to the reaction that was irradiated, analysis by GC showed only starting materials with no formation of desired product **5a**, and metal hydride **1a** was again observed by NMR

spectroscopy. Further heating of the reaction also failed to give product **5a** (Table 1, entry 2). Using HBpin gave similar results to the reaction with  $B_2Pin_2$ . Only HBpin was visible in the GC trace and complex **1a** was the only metal complex in the  $^1H$  NMR spectra (Table 1, entry 3). Note that stoichiometric activation of neat HBpin with the  $PM_3$  substituted version of **1** has been investigated previously, showing B-H oxidative addition to give  $Tp'Rh(PM_3)(Bpin)H$  [26].

**Table 1**

Screen of benzene borylation with trispyrazolylborate complexes.

Entry	$B_2Pin_2$ equiv	HBpin equiv	<b>5</b> equiv	Catalyst	Conversion <sup>a</sup> of $B_2Pin_2/HBpin$
					5
1 <sup>b</sup>	1	-	230	1	0%
2 <sup>c</sup>	1	-	284	1	0%
3 <sup>c</sup>	-	1	286	1	0%
4 <sup>d</sup>	1	-	106	2	~30%
5 <sup>c</sup>	-	1	197	2	~40%
6 <sup>e</sup>	1	-	91	3	~36%
7 <sup>f</sup>	1	-	4	3	~95%
8 <sup>g</sup>	-	1	93	3	~62%
9 <sup>g</sup>	1	-	77	4	~40%
10 <sup>g</sup>	-	1	77	4	~98%

<sup>a</sup>Conversion of borylating agent to  $PhBpin$  based on area ratios of GC peaks, no internal standard used, qualitative conversion.

<sup>b</sup>Irradiated at RT for 5 h. <sup>c</sup>Heated at 115 °C for 4 h. <sup>d</sup>Heated at 110 °C for 4 d. <sup>e</sup>Heated at 115 °C for 24 h. <sup>f</sup>Heated at 120 °C for 3 d in 1.5 mL *n*-octane. 37 % conversion after 24 h.

<sup>g</sup>Heated at 115 °C for 3 h.

## 2.2. Borylation with $Tp'Rh(CNR)_2$

We next examined catalysis using complex **2**. Borylation of benzene was attempted thermally at 130 °C for 5d [27]. Catalysis with complex **2** led to a 20% consumption of  $B_2Pin_2$  and GC showed a newly formed peak corresponding to product **5a** (Table 1, entry 4). Borylation using HBpin resulted in a much faster reaction, with just over 50% of HBpin consumed and the desired product **5a** observable by GC (Table 1, entry 5). Catalysis using **2** was attempted at lower temperatures but no reaction was observed at temperatures below 130 °C.

## 2.3. Borylation with $Tp'Ir(C_2H_4)_2$

From there, we began our investigation into the trispyrazolylborate ethylene complexes, starting with the iridium complex **3**. Running the reaction neat at 115 °C showed ~40% consumption of  $B_2Pin_2$  and a new peak corresponding to product **5a** in the GC trace (Table 1, entry 6). When octane was added as a solvent, the reaction showed 95% consumption of  $B_2Pin_2$  and the formation of product **5a**, although the reaction was very slow (Table 1, entry 7). Catalysis with HBpin showed a more rapid reaction when compared to the reaction of  $B_2Pin_2$  in neat benzene (Table 1, entry 6), giving 50% consumption of HBpin and detection of the product **5a** (Table 1, entry 8). In all cases, the yield of **5a** was not quantitative.

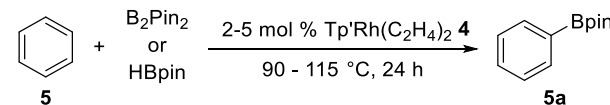
## 2.4. Borylation with $Tp'Rh(C_2H_4)_2$

Next, borylation of benzene using the corresponding rhodium complex  $Tp'Rh(C_2H_4)_2$  **4** was attempted. Initial conditions using an excess of benzene at 115 °C produced borylated product **5a** in a 76% isolated yield (Table 2, entry 1). Attempts at lowering

the number of equivalents of benzene and diluting the reaction with *n*-heptane resulted in poor yields (Table 2, entries 2-3). It was observed that the reaction with a lower loading of benzene (Table 2, entry 2) performed slightly better than the reaction with more benzene (Table 2, entry 3). This suggests that this transformation relies heavily on having an excess of one substrate. In entry 2 the boron to benzene ratio is 2:0.5 while in entry 3 the boron to benzene ratio is 1:1 (due to the fact that  $B_2Pin_2$  contains two equivalents of boron per molecule). Switching borylating agents from  $B_2Pin_2$  (Table 1, entry 1) to HBpin (Table 1, entry 4) gave slightly lower yields. This is likely due to the fact that 1 equivalent of each borylating agent was used, but  $B_2Pin_2$  provides double the equivalents of boron, manipulating the ratio of boron to benzene. HBpin was used for further optimization for ease of reaction set up. The temperature was able to be lowered to 100 °C without a loss in yield, but upon lowering the temperature to 90 °C a drastic reduction in yield was observed (Table 2, entry 6). The reaction, when scaled from 0.22 mmol scale to a 0.4 mmol scale, resulted in a slight increase in yield (Table 2, entries 5 & 10). Furthermore, the equivalents of benzene were lowered to 4 equiv without a loss in yield (Table 2 entries 10 & 11). It was seen when lowering the equivalents of benzene below four, a reduction in yield was observed (Table 2, entries 8,9, & 13). Specifically, reducing the amount of benzene to 2-3 equivalents, led to a 10% decrease in yield (Table 2, entries 9 & 13). A 1:1 ratio of substrates led to a drastic drop in yield to 30% (Table 1, entry 8).

**Table 2**

Borylation of benzene using  $Tp'Rh(C_2H_4)_2$  (**4**).



Entry	$B_2Pin_2$ equiv	HBpin equiv	<b>5</b> equiv	heptane mL	T °C	Yield <b>5a</b> <sup>b</sup>
1 <sup>a</sup>	1	-	76	-	115	76%
2 <sup>a,e,g</sup>	1	-	0.5	1.5	115	12%
3 <sup>a,e,h</sup>	1	-	2	1.5	115	5%
4 <sup>a</sup>	-	1	76	-	115	60%
5 <sup>a</sup>	-	1	4	-	100	73%
6 <sup>a</sup>	-	1	4	-	90	45%
7 <sup>c,e</sup>	-	2	1	-	100	6%
8 <sup>c</sup>	-	1	1	-	115	30%
9 <sup>c</sup>	-	1	2	-	100	69%
10 <sup>c</sup>	-	1	4	-	100	81%
11 <sup>c</sup>	-	1	20	-	115	80%
12 <sup>d</sup>	-	1	4	-	100	60%
13 <sup>c</sup>	-	1	3	-	100	70%
14 <sup>f,e</sup>	-	1	20	-	100	5%

<sup>a</sup>0.22 mmol scale, 5 mol % catalyst. <sup>b</sup> isolated yield. <sup>c</sup>0.4 mmol scale, 4 mol % catalyst. <sup>d</sup>0.4 mmol, 2 mol % catalyst. <sup>e</sup> NMR yield vs. dimethylsulfone as the internal standard. <sup>f</sup>Hg drop added, 0.4 mmol, 4 mol % catalyst, 0.81% of the doubly borylated product 1,3-bis(4,4,5,5-tetramethyl-1,3,2-dioxaborolan-2-yl)benzene was observed. <sup>g</sup>3.5% of the doubly borylated product 1,3-bis(4,4,5,5-tetramethyl-1,3,2-dioxaborolan-2-yl)benzene was observed. <sup>h</sup>7.4% of the doubly borylated product 1,3-bis(4,4,5,5-tetramethyl-1,3,2-dioxaborolan-2-yl)benzene was observed.

It was found that using an excess of the arene rather than boron source was critical for reactivity; an excess of HBpin reduced the yield from 69% to 6% (Table 2, entries 7 & 9). The catalyst loading was lowered from 5 mol % to 4 mol % without a reduction in yield, but upon lowering it further to 2 mol %, a

20% reduction in the yield of **5a** was observed. Final optimized conditions use a ratio of benzene to HBpin of 4:1, a catalyst loading of 4 mol %, and heating the reaction to 100 °C (Table 2, entry 10). Upon completion of a mercury drop test, a large decrease in yield was observed suggesting this system is catalyzed by Rh nanoparticles, which is something our group has seen previously with similar catalysts (Table 2, entry 14) [28]. Monitoring the reaction vs. time shows a smooth conversion to produce product **5a** with no induction period (see Supporting Information).

Further characterization by X-ray powder diffraction (XRD) showed a crystalline material that was a mixture of Rh metal and several different Rh oxides. We observed the Rh oxide formation in samples analyzed in air and samples analyzed under an inert atmosphere. This suggests that the Rh oxides are forming during the reaction. Additionally, transmission electron microscopy (TEM) was done showing the formation of 0.17  $\mu$ m Rh oxide aggregates and Rh metal nanoparticles (see Supporting Information for more details).

### 2.5. Borylation of toluene and anisole with $Tp'Rh(C_2H_4)_2$

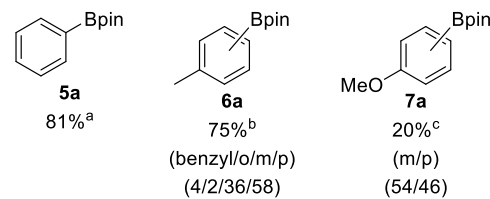
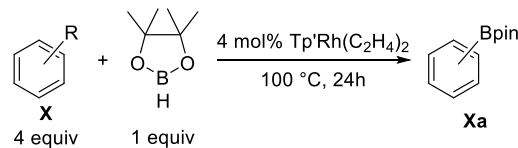
With optimizations in hand, we explored the effects of simple electron withdrawing and donating substitution on the arene ring. Fluorobenzene, chlorobenzene, anisole and toluene were submitted to the reaction conditions (Scheme 1). Reaction with chlorobenzene showed cleavage of the C-Cl bond, forming benzene and a mixture of the borylated chlorobenzene and **5a** in trace yield. Fluorobenzene was chosen to avoid the C-X bond cleavage and although it showed better reactivity than chlorobenzene the yield remained below 10%. Unfortunately introducing any functionality to the arene resulted in a drastic drop in yield under our optimized conditions. Substrates **6a**-**7a** worked best using a much larger excess of arene, specifically 18-20 equiv. Toluene was able to be borylated in a 75% yield when using a large excess of arene, however lowering the arene to 4 equiv resulted in over a 50% reduction in yield. Using a large excess of anisole did not give the same increase in yield compared to the reaction at 4 equiv. The reaction with 20 equiv of anisole gave a 20% combined yield of the *meta* and *para* products. The *ortho* isomer was observed by GC-MS, with a ratio for the o/m/p isomers of 4:49:47, but the *ortho* isomer was not able to be observed by NMR analysis.

### 2.6. Conclusions

In conclusion, four different trispyrazolylborate catalysts were investigated for direct arene borylation. Catalysts **3** and **4** showed the greatest reactivity out of all the catalysts, and further optimization using catalyst **4** allowed for the direct borylation of benzene to occur in 81% yield. Unfortunately, this methodology could not be extended to functionalization of other arenes. A drastic drop in yield is observed when simple functional groups are introduced, and this system does not tolerate electron withdrawing substitution on the arene. Although trispyrazolylborate catalysts **3** and **4** are isoelectronic to their pentamethylcyclopentadienyl counterparts, the same reactivity is not observed, and nanoparticle catalysis is indicated with rhodium. Also, complex **4** requires heating to 100 °C to effect borylation, whereas one of the best systems reported by Ishiyama, Miyaura, and Hartwig ( $[IrCl(COEt)_2]_2 + 4,4'$ -di-t-butylbipyridine) operates at room temperature [29, 30].

### Scheme 1

#### Substrate scope



<sup>a</sup>reaction run with 4 equiv of benzene at 100 °C for 24 h. <sup>b</sup>reaction run with 18 equiv of toluene at 115 °C for 21 h. <sup>c</sup>reaction run with 20 equiv of anisole at 100 °C for 24 h, NMR yield of *meta* and *para* products vs. dimethylsulfone as the internal standard

## 3. Experimental

### 3.1. General

All operations were performed under a nitrogen atmosphere, either in a Vacuum Atmosphere Corporation Glove Box or on a high vacuum line using modified Schlenk techniques. –

### 3.2. Reagents

Benzene-d<sub>6</sub> was purchased from the Cambridge Isotope Lab and distilled under vacuum from dark purple solutions of benzophenone ketyl and stored in ampoules with Teflon sealed vacuum line adaptors. Benzene and octane were purchased from Aldrich Chemical Co. and distilled from dark purple solutions of benzophenone ketyl (solvents for table 1). Anhydrous benzene and toluene were obtained from an Innovative Technology PS-MD-6 solvent purification system and were degassed by freeze-pump-thaw cycles and stored in a nitrogen glove box over 4 Å molecular sieves (solvents for table 2 and substrate scope). *n*-heptane was purchased from Sigma Aldrich and was degassed by freeze-pump-thaw cycles and stored over 4 Å molecular sieves. The following substrates were used without further purification: chlorobenzene (Oakwood), anisole (Sigma Aldrich), fluorobenzene (Sigma Aldrich)

### 3.3. Syntheses

Preparation of **KTp'** [31], **Tp'Rh(CNR)( $\eta^2$ -PhN=CNR)** (**1**) [32], **Tp'Rh(C<sub>2</sub>H<sub>4</sub>)<sub>2</sub>** [33], **Tp'Ir(C<sub>2</sub>H<sub>4</sub>)<sub>2</sub>** [34], and neopentylisocyanide (**L**) [35] have been previously reported.

### 3.4. Instrumentation

All <sup>1</sup>H NMR spectra were recorded on a Bruker AMX400 or Bruker AVANCE400 spectrometer and referenced using chemical shifts of residual solvent resonances (C<sub>6</sub>D<sub>6</sub>,  $\delta$  7.16). TEM imaging was ran on a FEI Tecnai F20 G2 scanning transmission electron microscope (S)TEM. All XRD data was collected using a Rigaku XtaLAB Synergy diffraction system using Mo/Cu radiation.

### 3.5. Photolytic Borylation of Benzene using $Tp'Rh(CNR)(\eta^2$ -PhN=CNR) (**1**) as the Catalyst (Table 1, entry 1).

A J. Young NMR tube was charged with 2.5 mg (0.0036 mmol, 5 mol %) of **1** and dissolved in 1.5 mL (16.8 mmol, 230 equiv) of benzene. To the solution was added at once, 18.6 mg (0.073 mmol, 1 equiv) of B<sub>2</sub>Pin<sub>2</sub>. The sample was irradiated for 10 min at room temperature, resulting in the bleaching of the

bright yellow solution. Under inert conditions, 1  $\mu$ L of the solution was drawn into a microsyringe and a GC trace was recorded immediately. The GC trace showed only the starting  $\text{B}_2\text{Pin}_2$  and no formation of **5a**. Irradiation for an additional 5 h did not result in the formation of any new products by GC. A  $^1\text{H}$  NMR spectrum of the mixture showed  $\text{Tp}'\text{Rh}(\text{CNR})(\text{C}_6\text{H}_5)\text{H}$  as the only metal complex.

### 3.6. Thermal Borylation of Benzene by $\text{B}_2\text{Pin}_2$ using $\text{Tp}'\text{Rh}(\text{CNR})(\eta^2\text{-PhN=CNR})$ (1) as the Catalyst

A J. Young NMR tube was charged with 2.0 mg (0.0029 mmol, 5 mol %) of **1** and dissolved in benzene.  $\text{B}_2\text{Pin}_2/\text{HBpin}$  was then added to the solution. The reaction was then heated in an oil bath at 115 °C. A GC trace, using a 1  $\mu$ L aliquot of the solution, was taken under inert conditions. No product was observed.

(Table 1, entry 2) benzene, 1.5 mL (16.8 mmol, 284 equiv),  $\text{B}_2\text{Pin}_2$ , 15 mg (0.059 mmol, 1 equiv). Heated for 4 h, no consumption of  $\text{B}_2\text{Pin}_2$  was observed by GC, and no peak corresponding to product **5a** was observed. The solution was heated for an additional 24 h, showing no change.

(Table 1, entry 3) benzene, 1.0 mL (11.2 mmol, 190 equiv), HBpin, 7.5 mg (0.059 mmol, 1 equiv). Heated for 4 h, no consumption of  $\text{B}_2\text{Pin}_2$  was observed by GC, and no peak corresponding to product **5a** was observed. The solution was heated for an additional 24 h, showing no change.

### 3.7. Borylation of Benzene using $\text{Tp}'\text{Rh}(\text{CNR})_2$ (2) as the Catalyst

A J. Young NMR tube was charged with 2.3 mg (0.0040 mmol) of **2** and dissolved in benzene.  $\text{B}_2\text{Pin}_2/\text{HBpin}$  was then added to the solution. The reaction was then heated in an oil bath. A GC trace, using a 1  $\mu$ L aliquot of the solution, was taken under inert conditions as described in the text.

(Table 1, entry 4) benzene, 0.75 mL (8.39 mmol, 106 equiv),  $\text{B}_2\text{Pin}_2$ , 20 mg (0.079 mmol, 1 equiv). Heated for 4 d at 110 °C, 20% consumption of  $\text{B}_2\text{Pin}_2$  was observed in the GC trace, along with a newly formed peak corresponding to product **5a**. GCMS: **5a**  $\text{M}^+$ , 204 m/z.

(Table 1, entry 5) benzene, 1.5 mL (16.8 mmol, 197 equiv), HBpin, 11 mg (0.085 mmol, 1 equiv). Heated for 4 d at 115 °C, 50% consumption of HBpin was observed in the GC trace along with a newly formed peak corresponding to product **5a**. GCMS: **5a**  $\text{M}^+$ , 204 m/z.

### 3.8. Borylation of Benzene by $\text{B}_2\text{Pin}_2$ using $\text{Tp}'\text{Ir}(\text{C}_2\text{H}_4)_2$ (3) as the Catalyst

A J. Young NMR tube was charged with 5.0 mg (0.0092 mmol, 5 mol %) of **3** and dissolved in benzene.  $\text{B}_2\text{Pin}_2/\text{HBpin}$  was then added to the solution. The reaction was then heated in an oil bath. A GC trace, using a 1  $\mu$ L aliquot of the solution, was taken under inert conditions.

(Table 1, entry 6) benzene, 1.5 mL (16.8 mmol, 91.2 equiv)  $\text{B}_2\text{Pin}_2$ , 46.5 mg (0.183 mmol, 1 equiv). Heated for 24 h at 115 °C, 40% consumption of  $\text{B}_2\text{Pin}_2$  was observed in the GC trace along with a newly formed peak corresponding to product **5a**. GCMS: **5a**  $\text{M}^+$ , 204 m/z.

(Table 1, entry 7) benzene, 32.9  $\mu$ L (0.368 mmol, 2 equiv),  $\text{B}_2\text{Pin}_2$ , 46.5 mg (0.183 mmol, 1 equiv), *n*-octane 1.5 mL (used as solvent). Heated for 72 h at 120 °C, 95% consumption of  $\text{B}_2\text{Pin}_2$  was observed in the GC trace along with a newly formed peak corresponding to product **5a**. GCMS: **5a**  $\text{M}^+$ , 204 m/z.

(Table 1, entry 8) benzene, 1.5 mL (16.8 mmol, 93.2 equiv), HBpin, 23 mg (0.180 mmol, 1 equiv), catalyst **3**, 4.9 mg (0.009

mmol, 5 mol %). Heated for 3 h at 115 °C, 50% consumption of HBpin was observed in the GC trace along with a newly formed peak corresponding to product **5a**. GCMS: **5a**  $\text{M}^+$ , 204 m/z.

### 3.9. Borylation of benzene using $\text{Tp}'\text{Rh}(\text{C}_2\text{H}_4)_2$ (4).

In a glovebox a J. Young NMR tube was charged with catalyst **4**, benzene and borylating reagent (HBpin/ $\text{B}_2\text{Pin}_2$ ). The reaction was then removed from the glovebox and placed in a metal heating block for 24 h. After 24 h, the reactions were allowed to cool to room temperature. Once cool, the reactions were diluted with dichloromethane (1 mL) and transferred to a scintillation vial. An additional 9 mL of dichloromethane was used to rinse the NMR tube and the washings were added to the scintillation vial. A GCMS of the crude reaction mixture was then recorded. The reaction was then worked up using a celite/silica plug. The plug was made out of a 30 mL syringe with a needle on the bottom. A glass fiber filter was placed in the bottom of the syringe and 10 mL of celite was added; the celite was packed with dichloromethane. Silica (3 mL) was added on top of the celite (to remove the decomposed catalyst) and was also packed with dichloromethane. The reaction mixture was then loaded onto the plug and the product was eluted with 200 mL of dichloromethane. The product was concentrated on a rotovap and further dried under vacuum overnight.

For reactions with an NMR yield the same workup was followed. Then once the reaction was fully concentrated, dimethylsulfone was added as an internal standard before taking the NMR spectrum.

(Table 2, entry 1) catalyst **4**, 5 mg (5 mol %), benzene, 1.5 mL (16.8 mmol, 76.3 equiv),  $\text{B}_2\text{Pin}_2$ , 55.8 mg (0.22 mmol, 1 equiv). 115 °C. Spectroscopic data for product **5a** matched the literature [36].  $^1\text{H}$  NMR (400 MHz,  $\text{CDCl}_3$ )  $\delta$  7.81 (d,  $J$  = 6.8 Hz, 2H), 7.46 (t,  $J$  = 7.2 Hz, 1H), 7.37 (t,  $J$  = 7.2 Hz, 2H), 1.35 (s, 12H).

(Table 2, entry 2) catalyst **4**, 5 mg (5 mol %), benzene, 9.8  $\mu$ L (0.11 mmol, 0.5 equiv),  $\text{B}_2\text{Pin}_2$ , 55.8 mg (0.22 mmol, 1 equiv), *n*-heptane 1.5 mL (solvent), 115 °C. Spectroscopic data for product **5a** matched the literature [36].

(Table 2, entry 3) catalyst **4**, 5 mg (5 mol %), benzene, 39.3  $\mu$ L (0.44 mmol, 2 equiv),  $\text{B}_2\text{Pin}_2$ , 55.8 mg (0.22 mmol, 1 equiv), *n*-heptane 1.5 mL (solvent), 115 °C. Spectroscopic data for product **5a** matched the literature [36].

(Table 2, entry 4) catalyst **4**, 5 mg (5 mol %), benzene, 1.5 mL (16.78 mmol, 76.3 equiv), HBpin, 31.9  $\mu$ L (0.22 mmol, 1 equiv), 115 °C. Spectroscopic data for product **5a** matched the literature [36].

(Table 2, entry 5) catalyst **4**, 5 mg (5 mol %), benzene, 78.6  $\mu$ L (0.88 mmol, 4 equiv), HBpin, 31.9  $\mu$ L (0.22 mmol, 1 equiv), 100 °C. Spectroscopic data for product **5a** matched the literature [36].

(Table 2, entry 6) catalyst **4**, 5 mg (5 mol %), benzene, 78.6  $\mu$ L (0.88 mmol, 4 equiv), HBpin, 31.9  $\mu$ L (0.22 mmol, 1 equiv), 90 °C. Spectroscopic data for product **5a** matched the literature [36].

(Table 2, entry 7) catalyst **4**, 7.3 mg (4 mol %), benzene, 35.7  $\mu$ L (0.4 mmol, 1 equiv), HBpin, 116  $\mu$ L (0.8 mmol, 2 equiv), 100 °C. Spectroscopic data for product **5a** matched the literature [36].

(Table 2, entry 8) catalyst **4**, 7.3 mg (4 mol %), benzene, 35.7  $\mu$ L (0.4 mmol, 1 equiv), HBpin, 58  $\mu$ L (0.4 mmol, 1 equiv), 115 °C. Spectroscopic data for product **5a** matched the literature [36].

(Table 2, entry 9) catalyst **4**, 7.3 mg (4 mol %), benzene, 71.5  $\mu$ L (0.8 mmol, 2 equiv), HBpin, 58  $\mu$ L (0.4 mmol, 1 equiv), 100 °C. Spectroscopic data for product **5a** matched the literature [36].

(Table 2, entry 10) catalyst **4**, 7.3 mg (4 mol %), benzene, 143  $\mu$ L (1.6 mmol, 4 equiv), HBpin, 58  $\mu$ L (0.4 mmol, 1 equiv), 100 °C. Spectroscopic data for product **5a** matched the literature [36].

(Table 2, entry 11) catalyst **4**, 7.3 mg (4 mol %), benzene, 0.715 mL (8 mmol, 20 equiv), HBpin, 58  $\mu$ L (0.4 mmol, 1 equiv), 115 °C. Spectroscopic data for product **5a** matched the literature [36].

(Table 2, entry 12) catalyst **4**, 3.6 mg (2 mol %), benzene, 143  $\mu$ L (1.6 mmol, 4 equiv), HBpin, 58  $\mu$ L (0.4 mmol, 1 equiv), 100 °C. Spectroscopic data for product **5a** matched the literature [36].

(Table 2, entry 13) catalyst **4**, 7.3 mg (4 mol %), benzene, 107  $\mu$ L (1.2 mmol, 3 equiv), HBpin, 58  $\mu$ L (0.4 mmol, 1 equiv), 100 °C. Spectroscopic data for product **5a** matched the literature [36].

(Table 2, entry 14) catalyst **4**, 7.3 mg (4 mol %), benzene, 0.715 mL (8.0 mmol, 20 equiv), HBpin, 58  $\mu$ L (0.4 mmol, 1 equiv), a drop of Hg, 100 °C. The Hg drop test was run using the same general procedure and workup described in the previous entries. Spectroscopic data for product **5a** matched the literature [36].

### 3.10. Functionalization of toluene using *Tp’Rh(C<sub>2</sub>H<sub>4</sub>)<sub>2</sub>* (4)

Catalyst **4**, 6.1 mg (3.9 mol %), toluene, 0.667 mL (6.27 mmol, 18 equiv), HBpin, 50  $\mu$ L (0.344 mmol, 1 equiv), 115 °C, 21h. Benzyl and *ortho* products were too small to be observed by <sup>1</sup>H NMR spectroscopy. 4,4,5,5-Tetramethyl-2-m-tolyl-1,3,2-dioxaborolane: Spectroscopic data for the meta product of **6a** matched the literature [36]. <sup>1</sup>H NMR (400 MHz, CDCl<sub>3</sub>)  $\delta$  7.67 (s, 1H), 7.64 (t, *J* = 4.4 Hz, 1H), 7.18-7.22 (m, 2H), 2.38 (s, 3H) 1.36 (s, 12H). 4,4,5,5-Tetramethyl-2-p-tolyl-1,3,2-dioxaborolane: Spectroscopic data for the para product of **6a** matched the literature [36]. <sup>1</sup>H NMR (400 MHz, CDCl<sub>3</sub>)  $\delta$  7.73 (d, *J* = 7.6 Hz, 2H), 7.29-7.30 (m, 2H), 2.38 (s, 3H) 1.37 (s, 12H).

### 3.10. Functionalization of anisole using *Tp’Rh(C<sub>2</sub>H<sub>4</sub>)<sub>2</sub>* (4)

Catalyst **4**, 7.3 mg (4 mol %), anisole, 0.869 mL (8.0 mmol, 20 equiv), HBpin, 58  $\mu$ L (0.4 mmol, 1 equiv), 100 °C. *Ortho* product was too small to be observed by <sup>1</sup>H NMR spectroscopy. 2-(4-methoxyphenyl)-4,4,5,5-tetramethyl-1,3,2-dioxaborolane: Spectroscopic data for the para product of **7a** matched the literature [37]. <sup>1</sup>H NMR (400 MHz, CDCl<sub>3</sub>)  $\delta$  7.76 (d, *J* = 8.7 Hz, 2H), 6.90 (d, *J* = 8.7 Hz, 2H), 3.83 (s, 3H), 1.35 (s, 12H). 2-(3-methoxyphenyl)-4,4,5,5-tetramethyl-1,3,2-dioxaborolane: Spectroscopic data for the meta product of **7a** matched the literature [38]. <sup>1</sup>H NMR (400 MHz, CDCl<sub>3</sub>)  $\delta$  7.45 – 7.20 (m, 3H), 7.08 – 6.91 (m, 1H), 3.83 (s, 3H), 1.35 (s, 12H).

### 3.11. Preparation of nanoparticle samples

In a glovebox a J. Young NMR tube was charged with catalyst **4**, 7.3 mg (4 mol %), benzene, 143  $\mu$ L (1.6 mmol, 4 equiv), and HBpin, 58  $\mu$ L (0.4 mmol, 1 equiv). The reaction was then

removed from the glovebox and placed in a metal heating block at 100 °C for 24 h.

*Atmospheric work-up.* In a separate experiment, after 24 h, the reaction was allowed to cool to room temperature. Once cool, the reaction was diluted with dichloromethane (1 mL) and transferred to a scintillation vial open to the atmosphere. An additional 9 mL of dichloromethane was used to rinse the NMR tube and the washings were added to the scintillation vial. The crude reaction mixture was then added in 1 mL aliquots to an Eppendorf tube and spun down in a centrifuge for 5 mins. Once finished, the mother liquor was decanted and more crude reaction mixture was added. When all of the reaction mixture had been spun down, 1 mL aliquots of DCM were added, centrifuged down, and then decanted off 3 separate times to wash the pellet completely.

*Air free work-up.* In a separate experiment, after 24 h, the reaction was allowed to cool to room temperature. Once cool, the reaction was brought back into the glovebox and diluted with dichloromethane (1 mL) and transferred to a scintillation vial. An additional 9 mL of dichloromethane was used to rinse the NMR tube and the washings were added to the scintillation vial. The crude reaction mixture was then added in 1 mL aliquots to an Eppendorf tube, brought outside the glovebox spun down in a centrifuge for 5 mins. Once finished, the Eppendorf was returned to the glovebox, the mother liquor was decanted off and more crude reaction mixture was added. The Eppendorf was then brought outside of the glovebox to be spun down in the centrifuge again. When all of the reaction mixture had been centrifuged, 1 mL aliquots of DCM were added 3 separate times inside the glovebox, centrifuged down outside the glovebox, and decanted off inside the glovebox to wash the pellet completely.

### Acknowledgment

We thank the U.S. Department of Energy, Basic Energy Sciences (BES) Chemical Sciences, Geosciences, & Biosciences (CSGB) Division, for financial support (DE-SC0020230). The authors gratefully acknowledge funding from the U.S. Department of Energy (Grant. No. DE-SC0020230) for instrument usage and chemicals. T.A.D. was supported by a DOE grant (DE-SC0020230). M.D.R. was supported by an NSF grant (CHE-1762350). The NSF program is acknowledged for the purchase of an X-ray diffractometer (CHE-1725028). We would also like to thank David Brewster for all of his help with the TEM and XRD data analysis.

### Declaration of Competing Interest

The authors declare no competing financial interest.

### Appendix A. Supplementary data

The Supplementary data are available free of charge on the website at DOI: 10.1021/xxxxxxxx.

Detailed information regarding GC spectra, X-ray powder spectra and TEM images. (PDF)

### ORCID

William D. Jones: 0000-0003-1932-0963

Andrew J. Vetter: 0000-0002-0222-4900

Tarah A. DiBenedetto: 0000-0001-8861-0740

Mikhaila D. Ritz: 0000-0003-2358-470X

## References

\* Corresponding author.

E-mail address: jones@chem.rochester.edu

<sup>†</sup> Authors contributed equally to this work

[1] Z.H. Syed, Z. Chen, K.B. Idrees, T.A. Goetjen, E.C. Wegener, X. Zhang, K.W. Chapman, D.M. Kaphan, M. Delferro, O.K. Farha, Mechanistic insights into C–H borylation of arenes with organoiridium catalysts embedded in a microporous metal–organic framework, *Organometallics* 39 (2020) 1123–1133.

[2] A. Das, P.K. Hota, S.K. Mandal, Nickel-catalyzed  $C(sp^2)$ –H borylation of arenes, *Organometallics* 38 (2019) 3286–3293.

[3] I.A.I. Mkhald, J.H. Barnard, T.B. Marder, J.M. Murphy, J.F. Hartwig, C–H activation for the construction of C–B bonds, *Chem. Rev.* 110 (2010) 890–931.

[4] K.M. Waltz, X. He, C. Muhoro, J.F. Hartwig, Hydrocarbon functionalization by transition metal boryls, *J. Am. Chem. Soc.* 117 (1995) 11357–11358.

[5] K.M. Waltz, J.F. Hartwig, Selective functionalization of alkanes by transition-metal boryl complexes, *Science* 277 (1997) 211–213.

[6] H. Chen, H.; J.F. Hartwig, Catalytic, regiospecific end-functionalization of alkanes: rhodium-catalyzed borylation under photochemical conditions, *Angew. Chem. Int. Ed.* 38 (1999) 3391–3393.

[7] C.N. Iverson, M.R. Smith, Stoichiometric and catalytic B–C bond formation from unactivated hydrocarbons and boranes, *J. Am. Chem. Soc.* 121 (1999) 7696–7697.

[8] T. Ishiyama, J. Takagi, K. Ishida, N. Miyaura, N. Anastasi, J.F. Hartwig, Mild iridium-catalyzed borylation of arenes. High turnover numbers, room temperature reactions, and isolation of a potential intermediate, *J. Am. Chem. Soc.* 124 (2002) 390–391.

[9] T. Ishiyama, J. Takagi, J.F. Hartwig, N.A. Miyaura, Stoichiometric aromatic C–H borylation catalyzed by iridium(I)/2,2'-bipyridine complexes at room temperature, *Angew. Chemie* 41 (2002) 3056–3058.

[10] S.I. Kalläne, M. Teltewskoi, T. Braun, B. Braun, C–H and C–F bond activations at a rhodium(I) boryl complex: Reaction steps for the catalytic borylation of fluorinated aromatics, *Organometallics* 34 (2015) 1156–1169.

[11] T. Furukawa, M. Tobisu, N. Chatani, C–H functionalization at sterically congested positions by the platinum-catalyzed borylation of arenes, *J. Am. Chem. Soc.* 137 (2015) 12211–12214.

[12] M.A. Esteruelas, M. Oliván, A. Vélez, POP–rhodium-promoted C–H and B–H bond activation and C–B bond formation, *Organometallics* 34 (2015) 1911–1924.

[13] Y. Saito, Y. Segawa, K. Itami, Para-C–H borylation of benzene derivatives by a bulky iridium catalyst, *J. Am. Chem. Soc.* 137 (2015) 5193–5198.

[14] N.G. Léonard, M.J. Bezdek, P.J. Chirik, Cobalt-catalyzed  $C(sp^2)$ –H borylation with an air-stable, readily prepared terpyridine cobalt(II) bis(acetate) precatalyst, *Organometallics* 36 (2017) 142–150.

[15] K.M. Waltz, X. He, C. Muhoro, J.F. Hartwig, Hydrocarbon functionalization by transition metal boryls, *J. Am. Chem. Soc.* 117 (1995) 11357–11358.

[16] T. Dombray, C.G. Werncke, S. Jiang, M. Grellier, L. Vendier, S. Bontemps, J.-B. Sortais, S. Sabo-Etienne, C. Darcel, Iron-catalyzed C–H borylation of arenes, *J. Am. Chem. Soc.* 137 (2015) 4062–4065.

[17] Z.H. Syed, Z. Chen, K.B. Idrees, T.A. Goetjen, E.C. Wegener, X. Zhang, K.W. Chapman, D.M. Kaphan, M. Delferro, O.K. Farha, Mechanistic Insights into C–H Borylation of Arenes with Organoiridium Catalysts Embedded in a Microporous Metal–Organic Framework, *Organometallics* 39 (2020) 1123–1133.

[18] A. Ros, R. Fernández, J.M. Lassaletta, Functional group directed C–H borylation, *Chem. Soc. Rev.* 43 (2014) 3229–3243.

[19] H. Chen, S. Schlecht, T.C. Semple, J.F. Hartwig, Thermal, catalytic, regiospecific functionalization of alkanes, *Science* 287 (2000) 1995–1997.

[20] D.D. Wick, T.O. Northcutt, R.J. Lachicotte, W.D. Jones, Carbon–hydrogen and carbon–carbon bond activation of cyclopropane by a hydridotris(pyrazolyl)borate rhodium complex, *Organometallics* 17 (1998) 4484–4492.

[21] E. Gutiérrez-Puebla, Á. Monge, M.C. Nicasio, P.J. Pérez, M.L. Poveda, L. Rey, C. Ruiz, E. Carmona, Vinylic C–H bond activation and hydrogenation reactions of  $Tp^*\text{Ir}(\text{C}_2\text{H}_4)(\text{L})$  complexes, *Inorg. Chem.* 27 (1998) 4538–4546.

[22] M. Paneque, P.J. Pérez, A. Pizzano, M.L. Poveda, S. Taboada, M. Trujillo, E. Carmona, C–H activation reactions on Rh(I)–ethylene complexes of the hydrotris(3,5-dimethylpyrazolyl)borate ligand,  $Tp^*\text{Me}^2$ , *Organometallics* 18 (1999), 4304–4310.

[23] Paneque, M.; Taboada, S.; Carmona, E. C–H and C–S Activation of Thiophene by Rhodium Complexes: Influence of the Ancillary Ligands on the Thermodynamic Stability of the Products. *Organometallics* 1996, 15, 2678–2679.

[24] P.J. Pérez, M.L. Poveda, E. Carmona, Ethylene dimerization: an alternative route involving vinyl hydride intermediates, *J. Chem. Soc., Chem. Commun.* (1992) 8–9.

[25] W.D. Jones, E.T. Hessel, Photolysis of  $Tp^*\text{Rh}(\text{CN}-\text{Neopentyl})(\eta^2\text{-PhN:C:N-Neopentyl})$  in alkanes and arenes: kinetic and thermodynamic selectivity of  $[Tp^*\text{Rh}(\text{CN}-\text{Neopentyl})]$  for various types of carbon–hydrogen bonds, *J. Am. Chem. Soc.* 115 (1993) 554–562.

[26] B. Procacci, Y. Jiao, M.E. Evans, W.D. Jones, R.N. Perutz, A.C. Whitwood, Activation of B–H, Si–H, and C–F bonds with  $Tp^*\text{Rh}(\text{PMe}_3)$  complexes: Kinetics, mechanism, and selectivity, *J. Am. Chem. Soc.* 137 (2015) 1258–1272.

[27] W.D. Jones, E.T. Hessel, Synthesis and structures of rhodium isocyanide complexes containing an  $\eta^2$ -hydrotris(3,5-dimethylpyrazolyl)borate ligand, *Inorg. Chem.* 30 (1991) 778–783.

[28] L. Munjanja, H. Yuan, W.W. Brennessel, W.D. Jones, Synthesis, characterization, and reactivity of  $\text{Cp}^*\text{Rh}(\text{III})$  complexes having functional N,O chelate ligands, *J. Organomet. Chem.* 847 (2017) 28–32.

[29] T. Ishiyama, J. Takagi, K. Ishida, N. Miyaura, N.R. Anastasi, J.F. Hartwig, Mild iridium-catalyzed borylation of arenes. High turnover numbers, room temperature reactions, and isolation of a potential intermediate, *J. Am. Chem. Soc.* 124 (2002) 390–391.

[30] T. M. Boller, J.M. Murphy, M. Hapke, T. Ishiyama, N. Miyaura, J.F. Hartwig, Mechanism of the mild functionalization of arenes by diboron reagents catalyzed by iridium complexes. intermediacy and chemistry of bipyridine-ligated iridium trisboryl complexes, *J. Am. Chem. Soc.* 127 (2005) 14263–14278.

[31] S. Trofimenko, J.R. Long, T. Nappier, S.G. Shore, Poly(1-pyrazolyl)borates and their complexes, borane adducts of bases, and haloborane adducts of bases, *Inorg. Synth.* 12 (1970) 99–109.

[32] E.T. Hessel, W.D. Jones, synthesis and structure of rhodium complexes containing a photolabile  $\eta^2$ -carbodiimide ligand. 1,3-Dipolar cycloaddition of phenyl azide to  $Tp^*\text{Rh}(\text{CN})_2$  [ $Tp^* =$  hydrotris(3,5-dimethylpyrazolyl)borate], *Organometallics* 11 (1992) 1496–1505.

[33] P.J. Pérez, M.L. Poveda, E. Carmona, Does the facile inter- and intramolecular C–H bond activation by  $Tp^*\text{-Rh}$  Complexes proceed via  $\text{Rh}^I$  or  $\text{Rh}^{III}$  intermediates? *Angew. Chem., Int. Ed. Engl.* 34 (1995) 231–233.

[34] Y. Alvarado, O. Bouthy, E. Gutiérrez, A. Monge, M.C. Nicasio, M.L. Poveda, P.J. Pérez, C. Ruiz, C. Bianchini, E. Carmona, Formation of hydrido- $\eta^3$ -allyl complexes of Ir(III) by sequential olefinic C–H bond activation and C–C coupling of alkenyl and olefin ligands, *Chem. - A Eur. J.* 3 (1997) 860–873.

[35] R.E. Schuster, *Organic Synthesis*; Wiley: New York, 1973.

[36] J.W. Clary, T.J. Rettenmaier, R. Snelling, W. Bryks, J. Banwell, W.T. Wipke, B. Singaram, Hydride as a leaving group in the reaction of pinacolborane with halides under ambient grignard and barbier conditions. one-pot synthesis of alkyl, aryl, heteroaryl,

---

vinyl, and allyl pinacolboronic esters, *J. Org. Chem.* 76 (2011) 9602–9610.

[37] M. Tobisu, R. Nakamura, Y. Kita, N. Chatani, Rhodium-catalyzed reductive cleavage of carbon–cyano bonds with hydrosilane: A catalytic protocol for removal of cyano groups, *J. Am. Chem. Soc.* 131 (2009) 3174–3175.

[38] K.L. Billingsley, S.L. Buchwald, An improved system for the palladium-catalyzed borylation of aryl halides with pinacol borane. *J. Org. Chem.* 73 (2008) 5589–5591.